

EXPERIMENTS OF TOMOGRAPHY-BASED SAR TECHNIQUES WITH P-BAND POLARIMETRIC DATA

F. Lombardini and M. Pardini
University of Pisa

Department of “Ingegneria dell’Informazione: Elettronica,
Informatica, Telecomunicazioni”

January 29th, 2009

Outline

Presentation of tomography-based coherent SAR data combination experiments and techniques with P-band airborne forest data regarding:

- Adaptive 3D SAR Tomography (Tomo-SAR)
- Principle of application of common band filtering to Tomo-SAR
- Sub-canopy DTM estimation

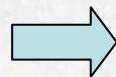
- Principle of coherent layer cancellation

- Radiometrically stabilized adaptive Polarimetric SAR Tomography (PolTomo-SAR)

Tomo-SAR as a spectral estimation problem

- **SAR Tomography** is a (non-model based) technique for the direct imaging (profiling) of elevation-distributed scatterers (semitransparent volume scattering layers) or layover scatterers
- Given the correspondence between heights and spatial frequencies, the tomographic h -profiling can be recast into a **spatial spectral estimation problem** along the height

N repeated flight tracks



Multibaseline (MB) cross-track array with N phase centers

height

$$\mathbf{a}(h) = [e^{jk_{z,1}h} \quad e^{jk_{z,2}h} \quad \dots \quad e^{jk_{z,N}h}]^T$$

Vertical wavenumber

Spatial steering vector

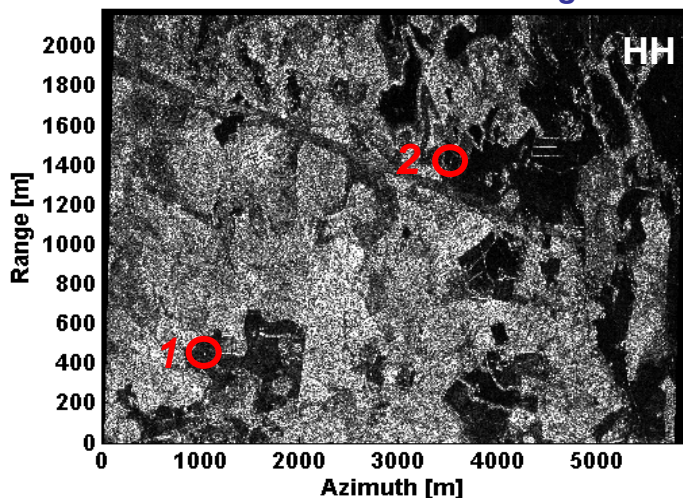
Array response to a backscattering signal component coming from height h

Non-parametric spectral estimation methods:

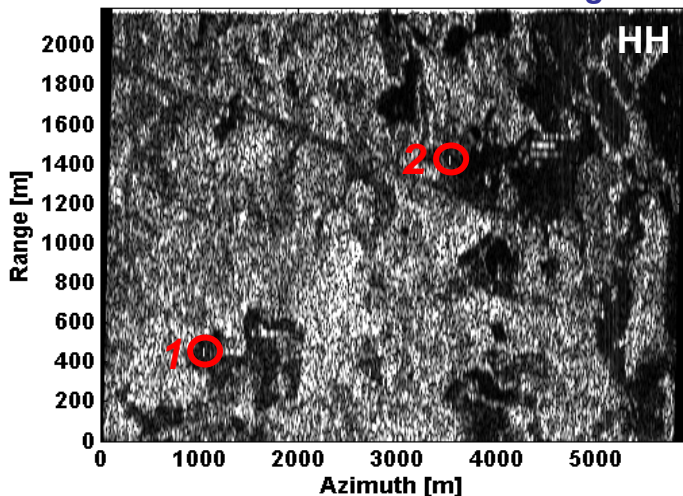
- **Beamforming:** classical Fourier imaging (multilook periodogram)
- **(Stabilized) Adaptive beamforming:** data adaptive null setting, resulting in height superresolution and sidelobe suppression capabilities

The BioSAR dataset

Full resolution SAR image

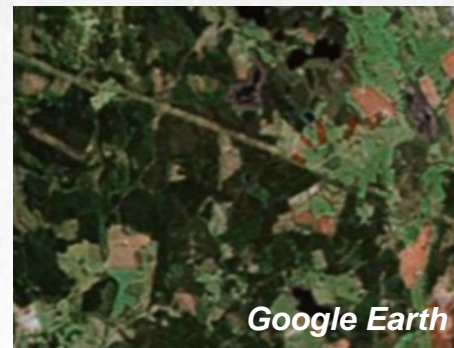


Emulated satellite SAR image

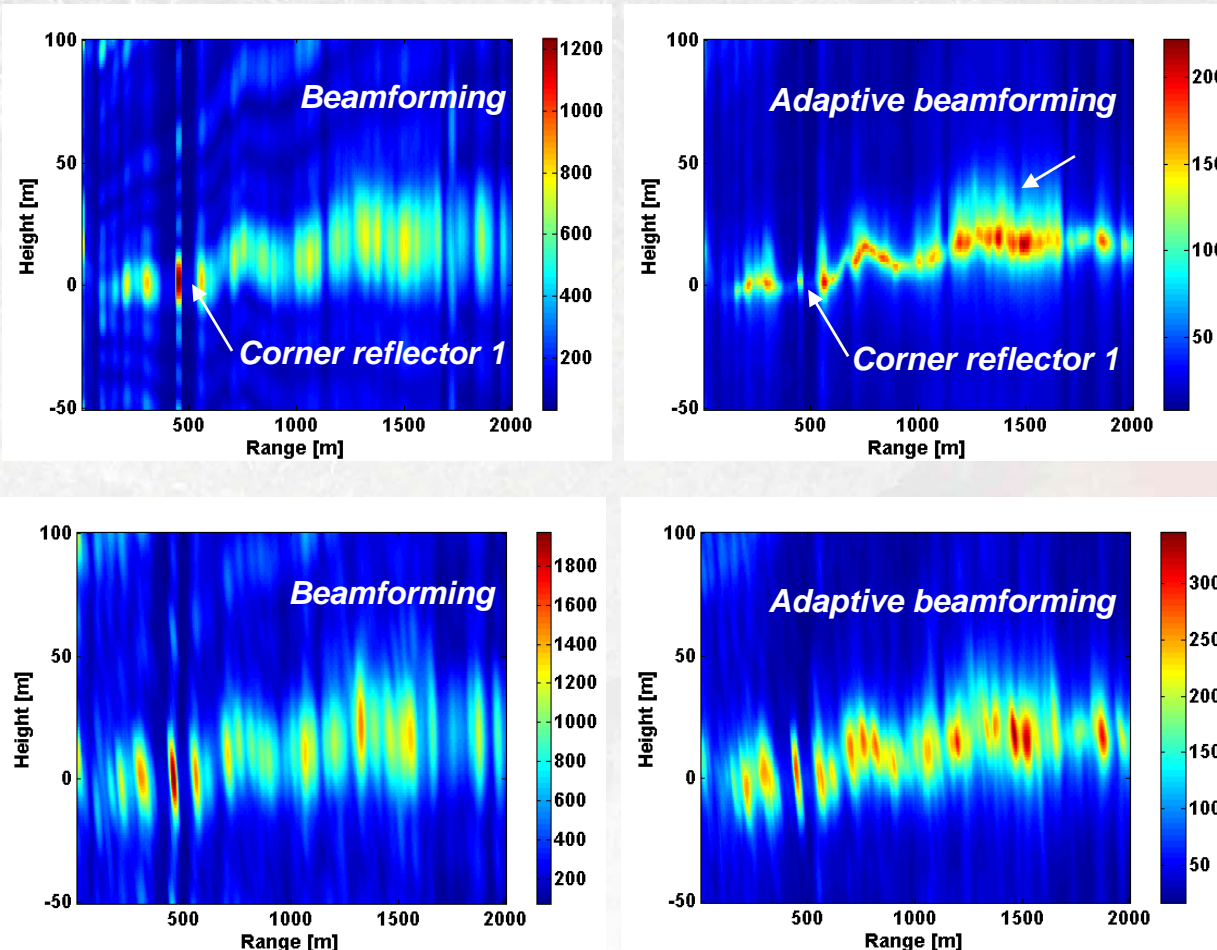


○ = Trihedral corner reflectors

- Airborne P-band acquisition campaign over the Remningstorp site (Sweden), March-May 2007, DLR E-SAR (ESA BioSAR project)
- 9 fully polarimetric images have been selected for processing, 80m horiz. total baseline
- Nominally uniform baselines
- Image resolution degraded to emulate the satellite resolution (6MHz, 25m rg x 11m az)
- Tomo cell: 50m ground rg (at near range) x 50m az (4 looks)
- HH expected more sensitive to terrain (double bounce terrain-tree trunks) than to canopy; conversely for HV
- Phase data re-calibration, PoliMi



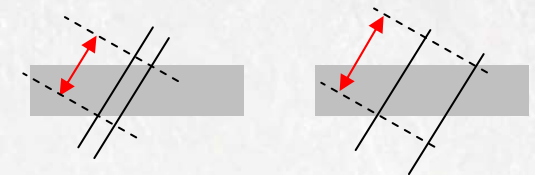
Examples of tomographic slices (HH)



Full resolution data

- Adaptive tomography can distinguish between terrain and canopy scattering
- self-cancellation, radiometric non-linearity

Emulated satellite data



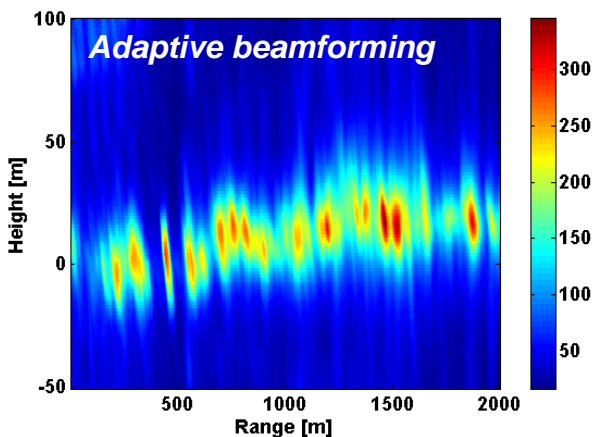
- Geometric perspective effects due to the poor range resolution widens and mixes the layers

Common band adaptive tomography (HH)

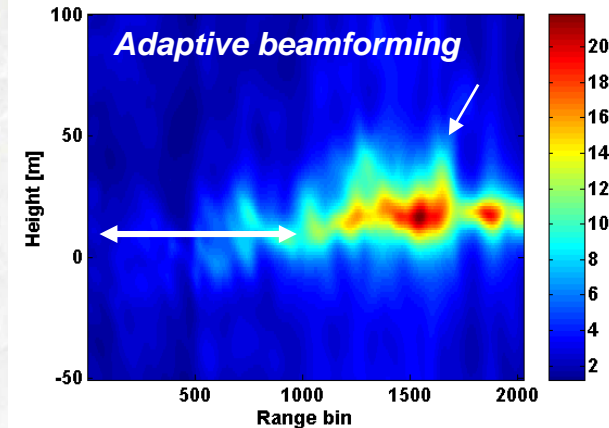
- To mitigate the detrimental geometric perspective effects affecting the tomographic processing with low resolution satellite data, a *common band pre-filtering* can be of help at the cost of a reduced ground range resolution

← [Gatelli *et al.*, TGARS '93]

A surface scatterer is widened by perspective effects; pre-filtering reduces the baseline decorrelation; hence, perspective effects have been reduced. This stands also for the various “sheets” in a volume.



Satellite data
Perspective effects are visible



Pre-filtering of satellite data
(2MHz)
The selected common bandwidth is available for all the images in mid to far range

With larger bandwidth data the selected common bandwidth for pre-filtering would be available for all the images at all ranges

Other adaptive tomography issues

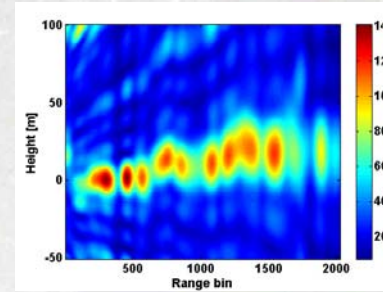
Robustness to the non-uniform baseline distribution

7 strongly non-uniform baselines have been selected from the 9 available (nominally uniform)

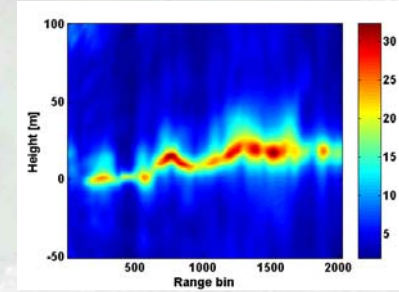
Self-cancellation phenomenon due to residual miscalibration and low number of looks

Uniform baselines

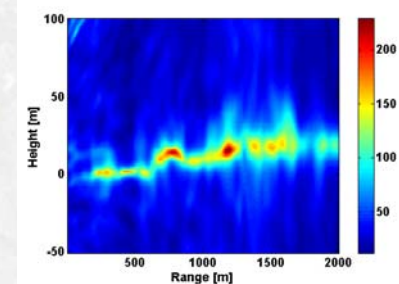
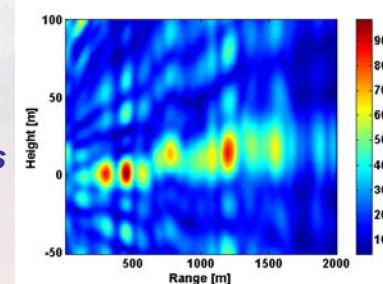
Beamforming



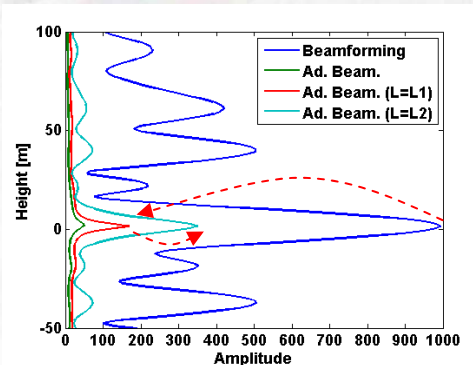
Adaptive beamforming



Non-uniform baselines



Example: corner 1, uniform

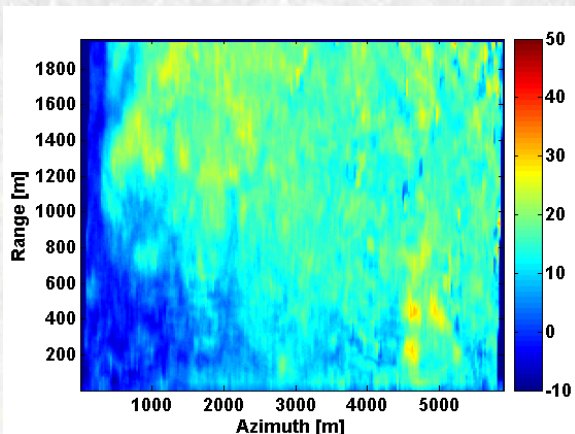


By augmenting the stabilization factor L , adaptive beamforming progressively recovers the radiometric linearity

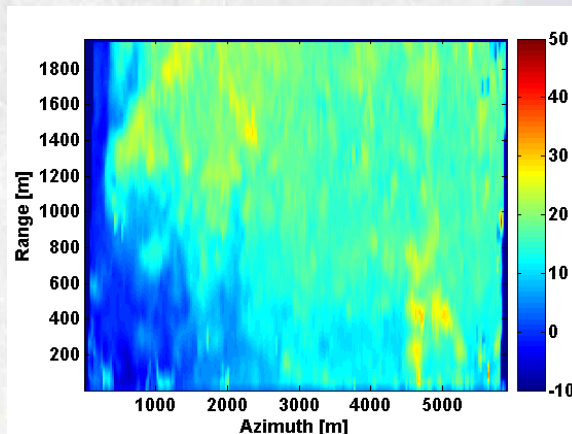
Sub-Canopy DTM estimation

HH: double bounce terrain-tree trunks + semi-transparent canopy

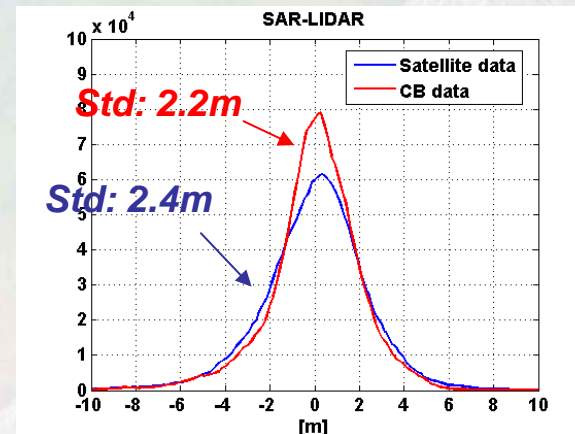
The DTM can be estimated by extracting the height of the most powerful peak of the adaptive spectrum



HH, satellite data



HH, pre-filtered data

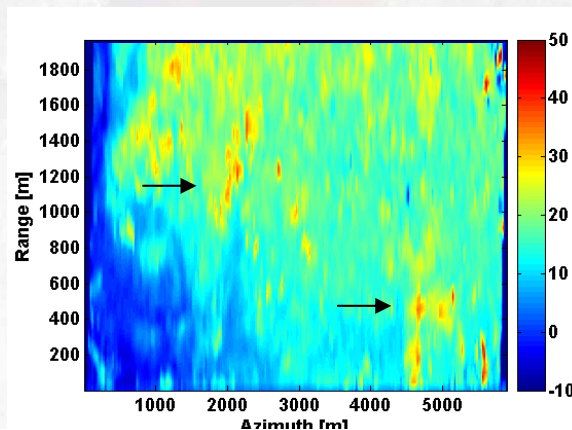


Validation with LIDAR: error histogram

HV data are less sensitive to double bounce; canopy is more powerful

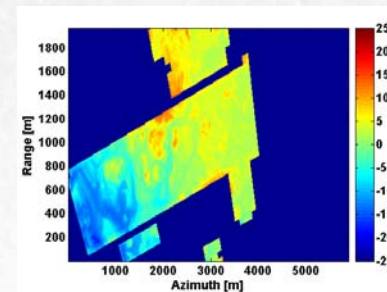


The resulting std after validation amounts to 3m, higher than the HH case



HV, pre-filtered data

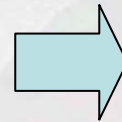
LIDAR DTM



Coherent layer canceller

- **Objective:** obtain a new complex MB dataset with only the height scattering components of interest for a given application and the others rejected
- **Solution:** design of a multiband filter with a pass and a stop band in height to process the multibaseline data vector at each rg-az coordinate

- possible non-uniform baselines make a FIR filter design atypical
- a moving window processing of the short data sequence would be subject to transient effects and height array resolution losses



Design of a **matrix filter**

Filtered MB data vector $\longrightarrow y_c = \mathbf{H}y$ \longleftarrow MB original data vector

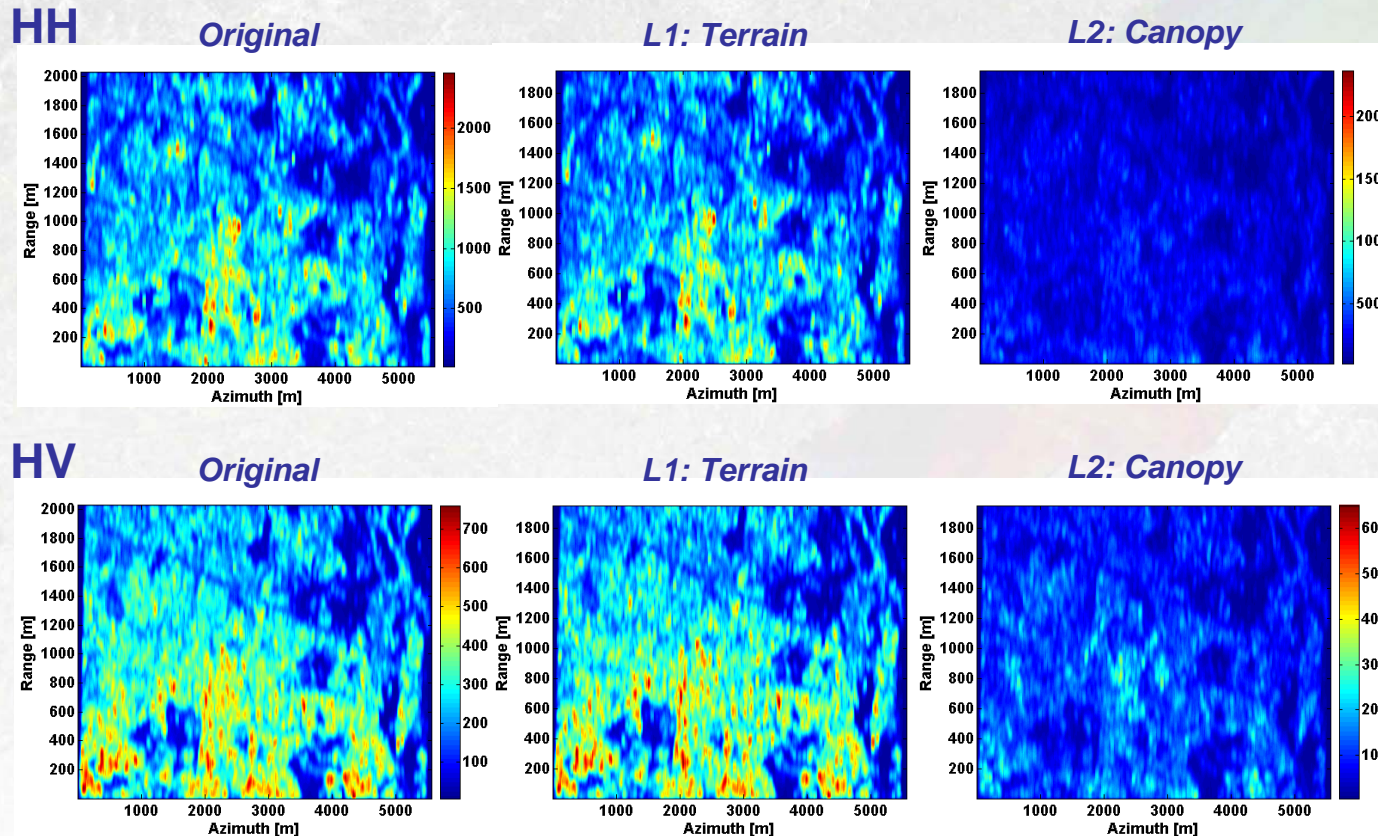
$$\mathbf{H} = \arg \min_{\mathbf{H}} \left(\underbrace{\int_{S_1} \|\mathbf{a}_V(h) - \mathbf{H}\mathbf{a}(h)\|^2, dh}_{\text{Leave unaltered the spatial harmonics in the pass band } S_1} + \underbrace{\int_{S_0} \|\mathbf{H}\mathbf{a}(h)\|^2, dh}_{\text{Reject as much as possible the spatial harmonics in the stop band } S_0} \right)$$

The output data structure can be different from the input one

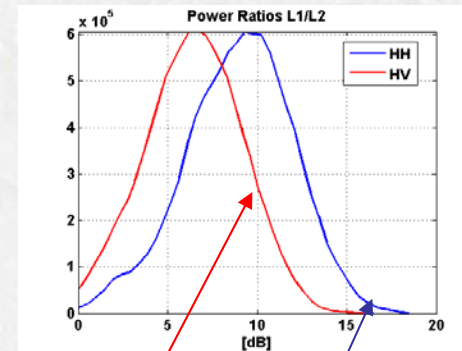
A regularization can be also used

Application of the coherent canceller: Layers reflectivity estimation

- Terrain layer centroid driven by the estimated DTM



MB incoherently averaged, 4 looks



Mean HV: 5.9dB

Mean HH: 7.2dB

Stabilized PolTomo adaptive beamforming processor

PolTomo extracts at the same time the height information of the multiple scatterers and a set of normalized complex coefficients describing the polarimetric scattering mechanism with fully polarimetric MB data

Fully polarimetric MB data vector (Pauli basis):

$$y_P = \begin{bmatrix} y_{HH} + y_{VV} \\ 2y_{HV} \\ y_{HH} - y_{VV} \end{bmatrix}$$

Normalized scattering coefficients (complex amplitude of each element of the Pauli basis):

$$\mathbf{k} = \begin{bmatrix} k_1 \\ k_2 \\ k_3 \end{bmatrix}$$

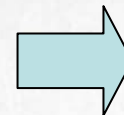
Spatial Polarimetric steering vector:

$$\mathbf{b}(h, \mathbf{k}) = \begin{bmatrix} k_1 \mathbf{a}(h) \\ k_2 \mathbf{a}(h) \\ k_3 \mathbf{a}(h) \end{bmatrix}$$

- *Single-pol beamforming and adaptive beamforming have been extended to estimate the scattering mechanism (closed form solution)*

[Sauer, Ferro-Famil, Reigber, Pottier, EUSAR 2008]

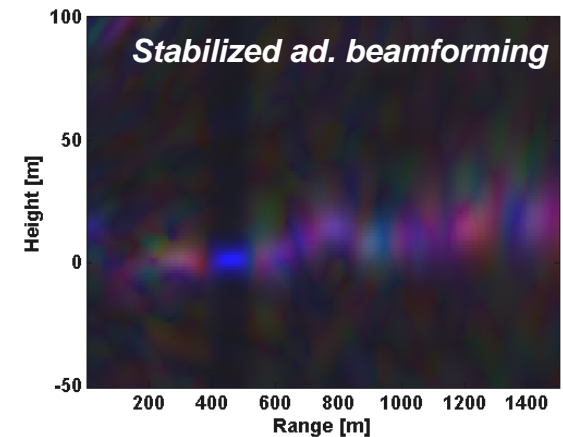
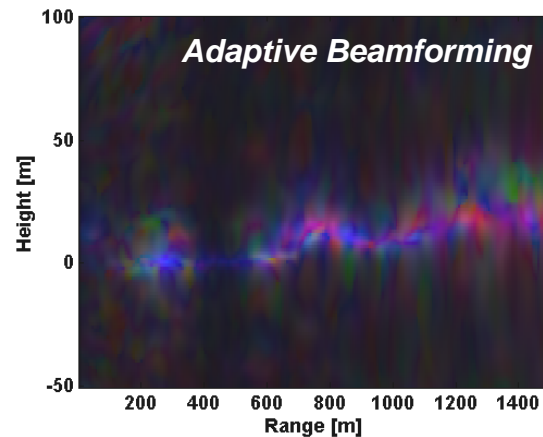
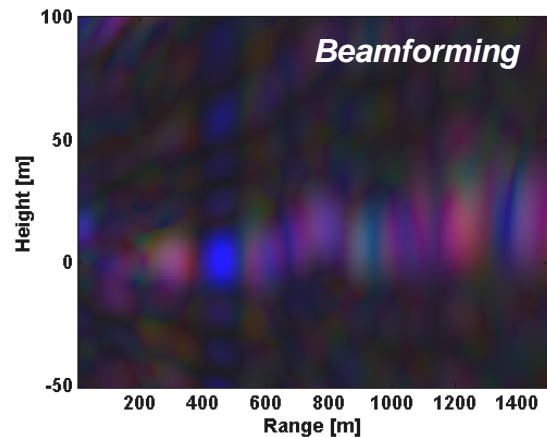
Problem: *possible radiometric unbalances between the output channels with PolTomo adaptive beamforming, due to self cancellation*
 → *k-estimation errors*



Proposed Solution: *including a stabilization factor!*

No closed form solution, an optimized grid search is needed

Examples of stabilized PolTomo slices: prefiltered data

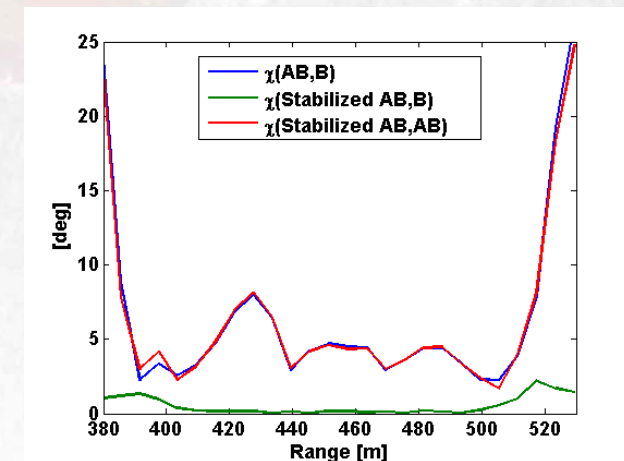


R: even bounce (e.g. double bounce)

G: random volume (e.g. canopy)

B: odd bounce (e.g. bare soil, trihedral corner reflectors)

- Comparison with the linear, but low resolution beamforming
- Non-linearity well recovered, at least in the single layer zones



Angular variations between vectors \mathbf{k} estimated with different methods (bare soil area)

Conclusions

- Adaptive processing can be powerful and flexible for Tomo-SAR
- Common band filtering can be of help in Tomo-SAR to reduce perspective effects
- Sub-canopy DTM can be extracted with Tomo-SAR
- Coherent layer cancellation can be performed, to possibly apply interferometric methods for single layer scenarios in two layer scenarios
- A stabilized adaptive PolTomo processor has been demonstrated to possess both good resolution in height and radiometric linearity between polarimetric channels

All the presented 3D tomography-based algorithms may be of interest also for future SAR spaceborne missions for biomass monitoring.